ARKIV FÖR FYSIK Band 18 nr 36

Communicated 1 June 1960 by Lise Meitner and G. Borelius

A fast chopper and its use in the measurement of neutron spectra

By E. Johansson, E. Lampa and N. G. Sjöstrand

With 14 figures in the text

SUMMARY

The fast chopper installed at the Swedish natural uranium–heavy-water reactor R1 is described. Its neutron properties as determined from measurements and calculations are discussed. The chopper has been used to measure the neutron spectrum in a beam from the central channel of the reactor. The beam was extracted from scatterers of water, heavy water, graphite or lead placed in various positions in the channel. It was found that the thermal spectrum can be fitted accurately to a Maxwell distribution. The epithermal spectrum from lead and graphite scatterers follows the $1/E$ law within 1 % in the region 2–10 eV but deviates from this law at higher energies, probably because of the resonance absorption in uranium. The shape of the function joining the Maxwell and $1/E$ parts together was studied in detail. The effective starting point of the $1/E$ spectrum was found to be $(3.6 \pm 0.4)\,kT$, where T is the neutron temperature. Supplementary measurements with foils and counters showed that the beam spectrum from graphite or lead scatterers is very closely the same as the spectrum in the empty channel. The neutron temperature in the channel was found to be 29 ± 10 degrees above the moderator temperature and the epithermal fraction β was obtained as 0.0420 ± 0.0015.

Introduction

Knowledge of the neutron spectrum in reactors is of great importance for all questions regarding neutron economy. Therefore a large amount of work has been devoted to calculations and measurements of reactor spectra.[1] However, a realistic calculation of the spectrum in an actual reactor involves such an enormous effort (even when the best available electronic computers are used) that severe approximations have to be made. It is also difficult to perform meaningful experiments. The uncertainties in the energy sensitivity of the spectrometer, backgrounds, etc. can usually be kept sufficiently low. More serious are the questions whether the spectrum in the neutron beam analysed by the spectrometer is the same as or different from the spectrum at the source point in the reactor, and whether the presence of a beam tube influences the reactor spectrum.

---

[1] A review of theoretical and experimental work has been given by Poole *et al.* [1]. More recent experiments have been described by Campbell *et al.* [2], Mostovoi *et al.* [3] and by Stone & Slovacek [4].

In spite of the interpretational difficulties expected, one of the first tasks for the fast chopper installed at the reactor R1 in the spring of 1958 has been the measurement of neutron spectra. The motivation is that rather few detailed measurements have been done so far, especially in the epithermal region and on heavy-water reactors. To be able to interpret the results, we have tried to vary the experimental conditions as much as possible at our reactor.

The first part of this article describes the chopper equipment. Its neutron properties are discussed in the second part. An account on spectrum measurements with the chopper is then given, and finally, complementary foil and counter experiments are described.

A. Fast chopper equipment

1. *General*

A general view of the equipment is given in Fig. 1. The neutron beam is extracted from a scatterer in the central vertical channel of the natural uranium–heavy-water reactor R1, which is located underground. The beam is limited in size by three collimator plugs in the top lids of the reactor, and it can be stopped by turning the upper plug 180 degrees. The beam can then pass through the chopper with its collima-

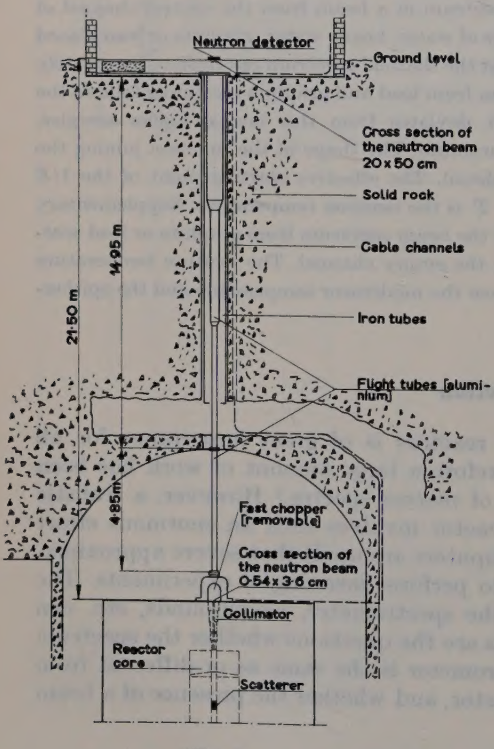

Fig. 1.

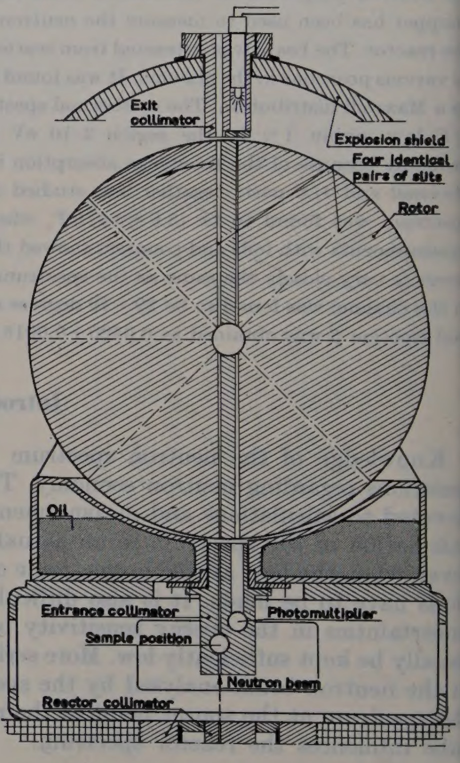

Fig. 2.

Fig. 1. A schematic view of the total experimental equipment.

Fig. 2. The rotor, collimators and start-pulse system.

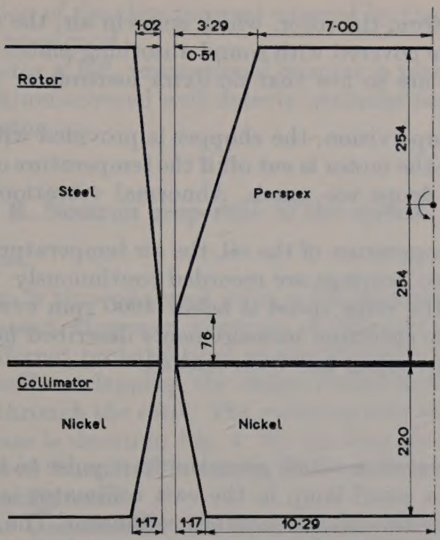

Fig. 3. The details of one chopper slit. For clarity the horizontal scale has been made much larger than the vertical in the figure. The dimensions are in mm.

tors. The flight path is about 21 m and consists of two evacuated aluminium tubes. It extends up to the ground level where a small house contains the detectors and the electronic equipment.

The chopper, with its driving mechanisms, was manufactured by the Rover Co. It is a modified version of the old Harwell fast chopper [5]. Together with the motors and other parts, it has been built in a compact unit which can be easily removed from the reactor top and replaced there.

2. *Rotor and driving system*

The rotor (shown in Fig. 2) has a diameter of 50.8 cm. Its thickness at the circumference is 4 cm and at the axis 25 cm. It was made from two chromium-nickel steel discs. In the flat surface of one of the discs, four grooves were made, 2.5 cm deep and 2 cm wide. Perspex inserts were placed in the grooves so that eight narrow slits were formed between the perspex and the steel. The details of one such slit are shown in Fig. 3. The narrowest part of a slit has the dimensions 0.051×2.54 cm^2. The two discs were then firmly bolted together to form the rotor, which has a weight of about 200 kg. The rotor is supported by ball bearings lubricated by circulating oil. Before delivery, the rotor was tested at speeds up to 11 500 rpm.

The rotor is driven by either of two induction motors. Rotor speeds from 1310 to 9390 rpm are obtained with a 20 hp motor and 196 to 1410 rpm with a 0.6 hp one. The low speeds are suitable for measurements on thermal neutrons. The extreme values of the half-width of the neutron burst are 2.0 μs and 98 μs.

3. *Shielding and control system*

The rotor is surrounded by an explosion shield of 5 cm thick steel. This has a weight of 600 kg and is fastened to the bottom plate by six bolts with a diameter of 3.7 cm.

To decrease the noise from the rotor, which spins in air, the openings on the sides of the explosion shield are covered with sound absorbing plates. The radiation levels on the top of the reactor are so low that no extra neutron or gamma-ray shielding is needed.

To avoid constant supervision, the chopper is provided with an automatic control system. The current to the motor is cut off if the temperature of the bearings is too high or if the oil pressure drops too much. Abnormal vibrations can also be made to cause a shut down.

The pressure and temperature of the oil, the air temperature near the rotor and the temperatures of the two bearings are recorded continuously. None of these temperatures exceeds 50°C if the rotor speed is below 4000 rpm even if the rotor is tightly sound-shielded. For the spectrum measurements described here, this speed has been sufficient, so no extra cooling has been needed.

4. *Start pulse system*

The principle for the system which gives the start pulse to the time-analyser is seen in Fig. 2. Light from a small lamp in the exit collimator is transmitted through a slit to a photomultiplier tube in the entrance collimator. The light flash occurs simultaneously with the neutron burst through the parallel slit. This simple system has been checked by measurements of the resolution function. It was found that geometrical imperfections in the rotor cause a negligible uncertainty in the starting times (see section B3).

5. *Detectors and electronic instrumentation*

The cross section of the neutron beam at the detector position is about 20×50 cm^2. Most of this area is covered by the neutron detector, usually a bank of BF_3 proportional counters. In the present measurements two different arrangements were used: either one layer of five BF_3 counters with diameter 3 cm and a BF_3 pressure of 30 mm Hg, or two such layers of similar counters, but with a BF_3 pressure of 600 mm Hg instead. The BF_3 was enriched in B^{10} to about 95%.

The detector pulses are fed into the time analyser. The time-selecting circuits were designed by J. Björkman, and the register belongs to a Philips 100-channel pulse-height analyser. The channel width can be varied in steps from 2 to 100 μs and the channels can be distributed in two groups with a time interval between them. A special arrangement allows the number of start pulses not followed by a detector pulse to be counted.

The analyser can only take one detector pulse per cycle, which means that corrections for pulse losses must be made. The correction factor for the ith channel is

$$p_i = S/(S - \sum_{\nu=0}^{i} N_\nu + \tfrac{1}{2} N_i),$$

where S is the total number of bursts and N_ν is the measured pulse number in the νth channel. The correction is apparently large for high channel numbers and low rotor speeds. With the lowest speed of the rotor, 196 rpm, the maximum value of p_{99} was about 1.7, which occurred at 0.0234 eV, the lowest energy of the present measurements. This correction may seem large, but it can be calculated very accurately, giving negligible contribution to the uncertainty of the measurements. It has been checked by variation of the time interval covered by the time analyser, and the agreement has always been good.

Below the chopper rotor a BF_3 proportional counter is placed as a monitor of the reactor flux. It is cadmium-covered and detects neutrons scattered from the beam by the entrance collimator.

B. Neutron properties of the system

1. *Transmission function*

When a $1/E$ spectrum is time-analysed using a $1/v$ detector, the counting rate per channel should be constant. However, neutrons of different speeds which enter the chopper slits have a different probability of passing through the slits without hitting the sides. In fact, to avoid overlapping, the chopper must not allow neutrons below a certain energy to pass through the rotor. The counting rate as a function of the time-of-flight for a typical case is shown in Fig. 4. We see that the cut-off occurs at about 80 % of the time between bursts. The empty interval in between can be used for measurement of the background.

In the ideal case, the transmission function depends only on the geometrical arrangements of the collimator and chopper slits and on the ratio of the neutron and rotor speeds. The function can be determined by measurements preferably in the epithermal region where, according to Fig. 4, the counting rate per channel is almost constant. The same energy region is then measured for two different rotor speeds. In order to get an extra check of the reliability of the determination we have usually made these measurements at three different rotor speeds. If the chopper has been removed from its position, the determination has to be repeated because minor changes may occur in the alignment of the system. In Table 1, the extreme values of the transmission correction for the present series of measurements are shown. The values have been arbitrarily normalized. From repeated measurements of the transmission function, we believe that the relative uncertainty in the transmission correction nowhere exceeds 2 %.

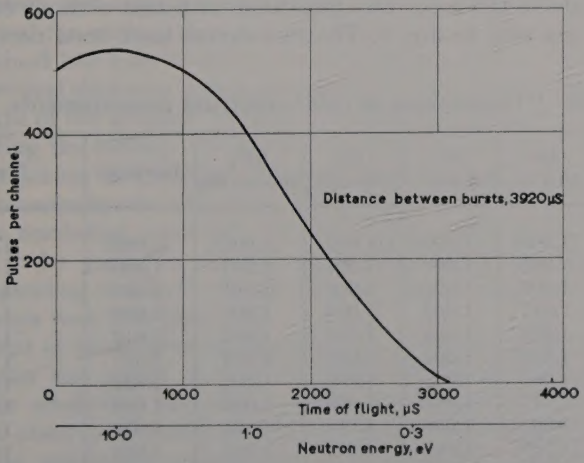

Fig. 4. A typical curve of the counting rate as a function of the flight time.

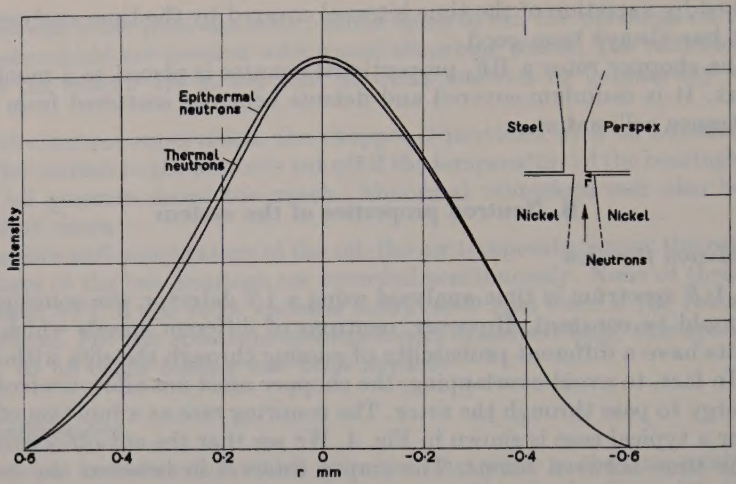

Fig. 5. The result of a static measurement of the pulse shape for thermal and epithermal neutrons.

The counting rate per μs channel width at the maximum of the curve in Fig. 4 is at a reactor power of 700 kW about 0.6 per min. This value refers to a detector of 10 BF_3 counters (see section A 5).

2. *Leakage*

The transmission function measured in the epithermal region is strictly applicable in the thermal region only if the leakage of neutrons through the walls of the slits is the same in both cases. Because the scattering cross section of the perspex walls varies with neutron energy, this is not so. In order to investigate the leakage, a static measurement was made. One of the rotor slits was adjusted to various positions relative to the slit in the entrance collimator by means of a micrometer screw, and the neutron intensity above the rotor was measured with and without cadmium in the beam. The results are seen in Fig. 5. The two curves have been normalized by cal-

Table 1. Corrections in total spectrum measurements.

t (μs)	E (eV)	Air 10.5 m	Al 6 mm	Cu 0.5 mm	BF_3 30 mm Hg	Leakage	Transmission
0		(1.000)	(1.000)	(1.000)	(1.000)	(1.000)	1.053–1.093
1000	2.34	1.000	1.000	1.000	1.001	1.000	1.031–1.070
2000	0.585	1.003	1.002	1.002	1.001	1.000	1.020–1.050
3000	0.260	1.017	1.003	1.003	1.002	1.000	1.010–1.037
4000	0.146	1.032	1.004	1.005	1.002	1.012	1.005–1.025
5000	0.0936	1.046	1.006	1.007	1.003	1.017	1.000–1.015
6000	0.0650	1.061	1.007	1.008	1.003	1.022	1.000–1.005
7000	0.0478	1.077	1.007	1.009	1.004	1.026	1.007–1.000
8000	0.0366	1.093	1.008	1.010	1.004	1.030	1.020–1.000
9000	0.0289	1.109	1.009	1.012	1.005	1.035	1.040–1.005
10000	0.0234	1.124	1.009	1.012	1.005	1.039	1.068–1.021

Table 2. Corrections in epithermal measurements.

t (μs)	E (eV)	Air 10.5 m	BF_3 600 mm Hg	Background
50	936	0.954	1.001	0.976
100	234	0.979	1.002	0.979
300	26.0	0.989	1.006	0.987
600	6.50	0.996	1.012	0.994
1000	2.34	1.000	1.020	1.000
1500	1.040	1.002	1.030	1.005
2000	0.585	1.003	1.041	1.007

culating the leakage in the case of perfect alignment of the slits ($r=0$). As expected, the leakage difference is larger at the perspex side. The area under the epithermal curve is 3 % larger than the area under the thermal one. This value has been used to evaluate the leakage corrections tabulated in Table 1. The relative error in the largest correction factor is probably not higher than 1 %.

The total leakage of neutrons in the epithermal region was roughly estimated as 15 % of the transmitted intensity.

3. *Energy calibration and resolution*

The distance from the chopping point to the middle of the detector is 21.16 m. Because the detector can be considered as thin, no correction is needed to take into account preferential stopping of neutrons in the front part of the detector. So the distance given is also the effective flight path of the neutrons within ±2 cm.

The energy of the neutrons (E) is related to the time-of-flight (t) as

$$E=\frac{2340\cdot 10^3}{t^2}\quad (E \text{ in eV, } t \text{ in } \mu\text{s}).$$

In order to obtain the correct time-of-flight, the readings from the time analyser must be corrected for various delays in the electronic equipment. The absolute time scale thus obtained has been tested by measurements of the positions of well-known resonances in several elements, and good agreement has always been found.

The half-width of the neutron burst at the highest possible rotor speed (9350 rpm) is 2.3 μs including the leakage. With the shortest channel width, 2 μs, this will give an optimum resolution of 0.15 μs/m. The largest half-width of the resolution function in the present measurements was about 150 μs used in the thermal region. At higher energies, better resolution was used, the best being a half-width of 10 μs, allowing measurements to be made on the flat epithermal spectrum down to flight times of 20 μs (corresponding to 6 keV). By calculations [4] it was shown that the resolution corrections always were less than 1 %.

A measurement of the resolution function was made using the 4.9 eV resonance in gold. The detector was placed close to the rotor, the speed of which was so low that the width of the resolution function was considerably larger than the width of the resonance. The observed resolution function agreed excellently with calculations, showing that no additional uncertainty arises from, for instance, the start-pulse system.

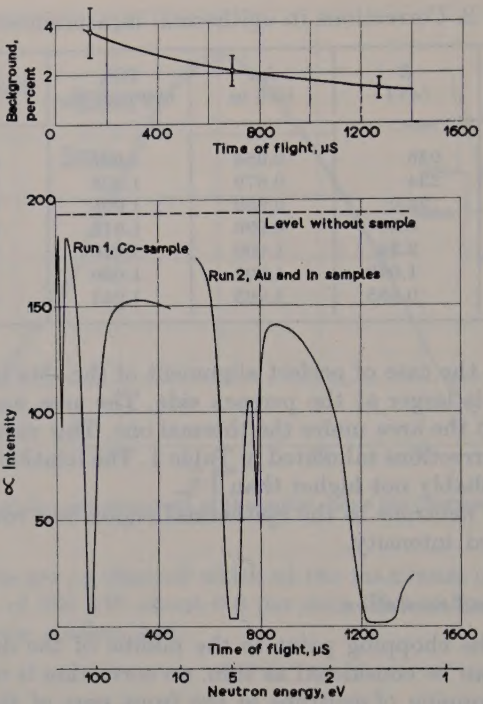

Fig. 6. The lower curve shows the intensity curves obtained with thick samples of Co, Au and In in the beam. The time-dependent background derived from these measurements is given in the upper curve.

4. *Background*

The background in the thermal region is less than 0.1 % and therefore negligible. In the epithermal region it is relatively higher and also time-dependent. This background is probably caused by burst neutrons which have collided with the walls of the flight path before reaching the detector. It has been measured with thick samples of indium, gold and cobalt which remove all neutrons of energies 1.46, 4.9 and 130 eV respectively, as shown in Fig. 6. The uncertainty in the background correction factor at the cobalt resonance is unlikely to be higher than 1 % and is smaller at lower energies.

5. *Neutron attenuation in flight path and detector*

On their way from the source to the detector, the neutrons have to pass through air, aluminium and copper. Because the cross sections of these substances vary with energy, small corrections must be made in spectrum measurements. Also the self-screening of the detector must be taken into account. These corrections are given in Tables 1 and 2. The measurements of the total neutron spectrum were made with the bank of five BF_3 counters and for the detailed measurements in the epithermal region, 10 counters in two layers were used (see section A 5).

C. Neutron spectrum measurements

1. *General arrangements*

Most chopper measurements were made with a scatterer in the middle of the reactor where the flux gradient is zero. Four scattterers of different materials were used: H_2O (height 20 cm), D_2O (11 cm), graphite (20 cm) and lead (3 cm). All four were cylindrical, fitting snugly into the central channel (inner diameter 15.4 cm). The epithermal spectrum has been measured in detail only with scatterers in the middle of the central channel, and these measurements were also used for the determination of the transmission function. Thermal spectrum measurements were also made with scatterers in various positions in the central channel.

Fig. 7 is a horizontal section through the central part of the reactor. The shaded area denotes the projection of the neutron detector on the scatterer at perfect alignment of the various parts of the system. Under ideal conditions only neutrons emitted from this area can reach the detector. In order to check this, measurements were made with a 0.5 mm thick cadmium sheet covering the scatterer. The result is given in Fig. 8. The neutron intensity in the thermal region is reduced to about 2 % of the value it has when the cadmium is not there. These neutrons can be accounted for by air-scattering and, to a smaller extent, by transmission through the cadmium. In view of the fact that they have a similar spectrum as the neutrons from the scatterer, they do not disturb our measurements. Thus the neutron spectrum observed in our chopper measurements refers to neutrons emitted from the scatterer.

The measurements were made with the reactor at highest possible power, 0.5 to 1 MW. A detailed measurement of the epithermal spectrum then takes about two days. For the thermal spectrum, a measuring time of about 15 hours is sufficient.

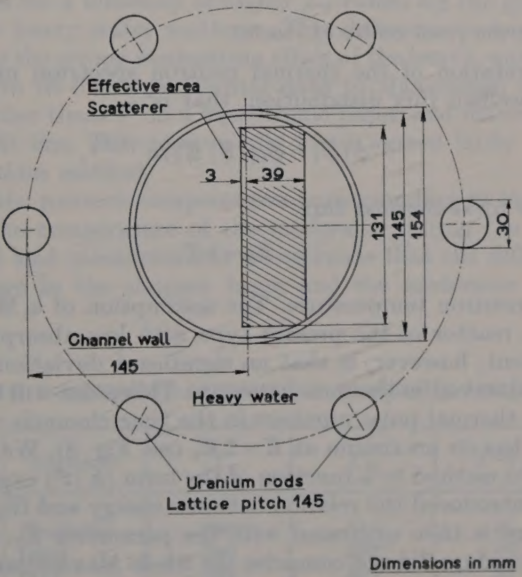

Fig. 7. A horizontal section through the central part of the reactor. The shaded area denotes the projection of the chopper detector on the surface of the scatterer.

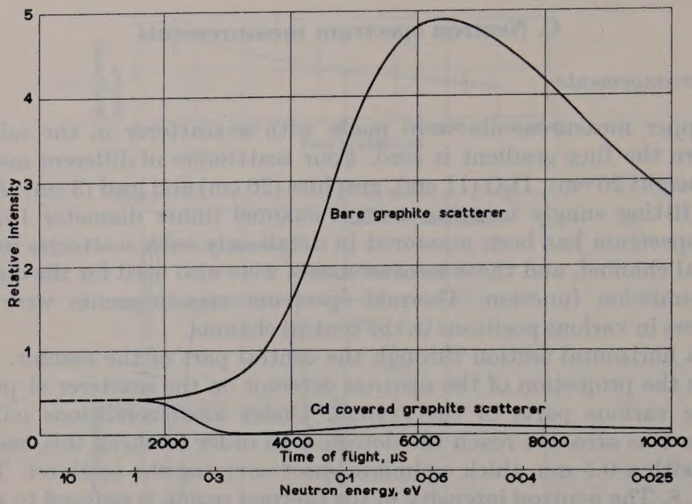

Fig. 8. Results from measurements with a bare and a cadmium-covered graphite scatterer. From the curves it is seen that practically all neutrons which reach the detector originate from the scatterer.

The pulse numbers obtained in the channels of the time analyser were corrected for counting losses, transmission function, leakage, and attenuation in the flight path and detector as described in section B. The numerical work was done with the help of the electronic computer BESK.

2. *Thermal spectrum from centre of reactor*

In the interpretation of the thermal neutron spectrum measurements we have assumed a Maxwellian flux distribution, that is

$$\phi(E) = \phi_{\mathrm{th}}(E/E_T^2)\,\mathrm{e}^{-E/E_T},$$

where ϕ_{th} is the total thermal flux.

$$E_T = kT,$$

where T is the neutron temperature. The assumption of a Maxwellian spectrum is reasonable for a reactor of the present type with low absorption and leakage. The strongest argument, however, is that no significant deviation from the Maxwellian shape has been observed in the measurements. This point will be discussed later.

The corrected thermal pulse numbers in the time channels will be proportional to $E^2 e^{-E/E_T}$ which has its maximum at $E = 2E_T$ (see Fig. 8). We have thus fitted them by a least-squares method to a function of the form $(K/t^4)\exp(-2340 \times 10^3/t^2 \times E_T)$ where we have introduced the relation between energy and flight time (t). The result of a measurement is then expressed with the parameter E_T.

The fitting procedure did not comprise the whole Maxwellian spectrum. At the low energy side, the cut-off in the measurements meant a loss of about 35 %. At the high energy side, the fitting must start at a reasonable distance from the epithermal region,

Table 3. The parameter E_T.

Run no.	Scatterer	Starting time, t_s (μs)		
		4500	5000	5500
110	Graphite	0.0297	0.0295	0.0294
115	Lead	0.0293	0.0292	0.0292
122	Heavy water	0.0290	0.0289	0.0289
129	Heavy water	0.0290	0.0287	0.0285

so that no error will be introduced from that part of the spectrum. To see the effect of this, the fitting was started at 4500, 5000 and 5500 μs (see Fig. 8) for four of the runs. This means that 60, 56 and 51 % respectively of the number of pulses for a complete Maxwellian distribution were used. The values of E_T thus obtained are given in Table 3.

We see that the E_T values with starting time $t_s = 4500$ μs are slightly higher than the others as would be expected if there was an influence of epithermal neutrons. It seems safe to assume that with $t_s = 5000$ μs, the contribution of epithermal neutrons cannot cause a larger uncertainty than about 1 % in E_T. Unless otherwise stated, we have used this value of t_s in all the least-squares fits mentioned later in this report.

Between the two heavy-water measurements, the chopper had been removed from the top of the reactor, so two independently determined transmission functions have been used in the evaluation of the data. The agreement between the E_T values obtained is an indication of the reproducibility of the measurements.

From Table 3 we also see a tendency of higher E_T values for the graphite and lead scatterers than for the heavy-water scatterer. This difference is hardly significant, but it may be caused by the strong moderating effect of the heavy-water scatterer.

We have also tried to fit our experimental data to Maxwellian distributions by plotting the pulse number times t^4 on a logarithmic paper and determining E_T from the slope of the straight line. This gave results which agreed fairly well with those found by the least-squares method.

In Table 4 we give the neutron temperatures corresponding to the E_T values for $t_s = 5000$ μs and also the temperature of the moderator during the measurements. From the graphite and lead measurements we estimate that the difference between the neutron temperature in the chopper beam and the moderator temperature is $29 \pm 6°$.

Table 4. Neutron temperature compared to moderator temperature.

Run no.	Scatterer	T	T_M	$T - T_M$
110	Graphite	342	311	31
115	Lead	339	312	27
122	D_2O	335	308	27
129	D_2O	333	310	23

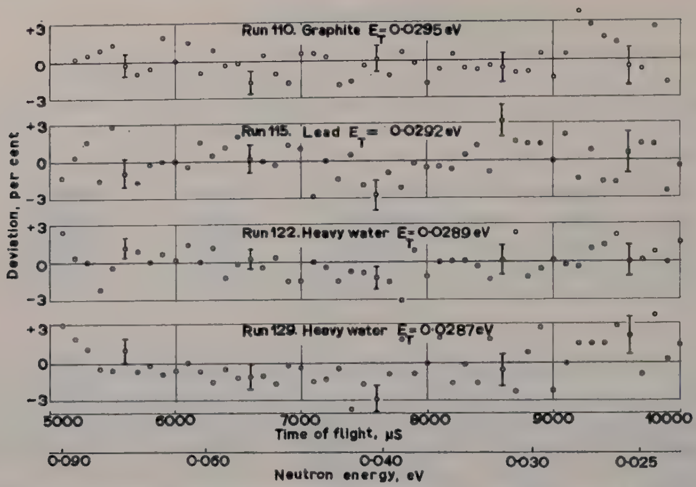

Fig. 9. The deviations of the measured pulse numbers from the computed Maxwellian functions. The figure gives four runs with the scatterer in the middle of the reactor.

Fig. 9 shows in detail how well the Maxwell spectrum can be fitted to the measured values. No significant deviation can be seen which is outside the typical statistical errors shown for a few points. This justifies our assumption of a Maxwell spectrum.

3. *Thermal spectrum from scatterers in different positions.*

By a 2 mm diameter steel wire it was possible to vary the position of the scatterer inside the central channel without moving the chopper or shutting down the reactor. The wire went through the opening in the reactor collimator, but it could not have

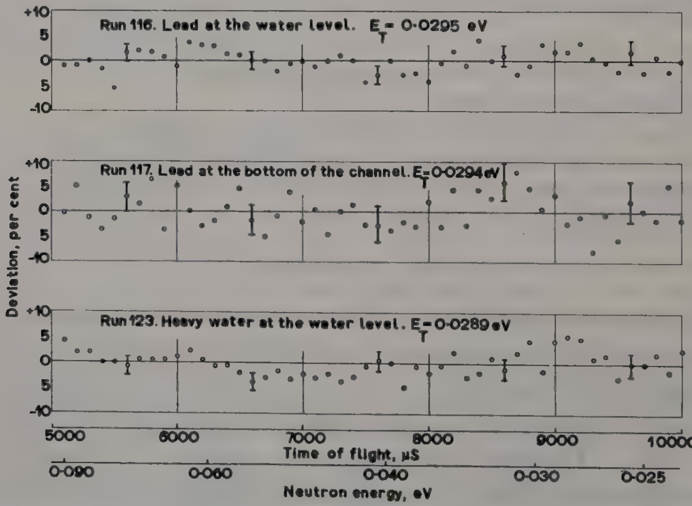

Fig. 10. The deviations of the measured pulse numbers from the computed Maxwellian functions for scatterers at the top or bottom of the reactor core.

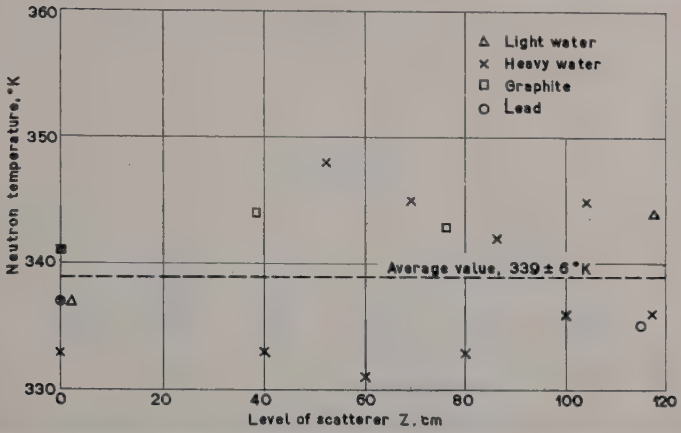

Fig. 11. Neutron temperatures at different scatterer positions normalized to a moderator temperature of 310°K.

had any disturbing effect on the measurements. In its top position, the scatterer had its upper surface approximately at the level of the heavy-water moderator. The lowest position was in the middle of the reactor, except for the lead scatterer which could also be placed at the bottom of the channel.

Fig. 10 shows the goodness of the fit of a Maxwellian flux to the spectra measured with the lead scatterer in its highest and lowest positions and with the heavy water scatterer in its highest position. The vertical flux gradient at the positions of the scatterers has been determined by copper wire activation as about 0.06 cm^{-1} (without any scatterer in the central channel). In no case is there any significant deviation from the Maxwellian shape.

Fig. 11 shows the neutron temperatures of all the spectra, measured with the scatterers in different positions (except one with the lead scatterer at the bottom of the channel). The abscissa in the figure is the distance from the middle of the reactor to the top of the scatterer. The heavy-water measurement giving higher values was less precise than the other measurement and was therefore not included in Table 4.

Fig. 11 indicates that there is no great difference in neutron temperature between various positions in the reactor.

4. *The epithermal spectrum*

The results from measurements of the epithermal spectrum from scatterers in the middle of the reactor are given in Fig. 12. The curves have been normalized to equal height in the thermal region. The graphite and heavy-water curves are each based on two independent measurements, whereas for lead and light water only one measurement was done. In the lead curve a correction has been done to remove the resonance dips of antimony, an impurity of the lead material.

It is apparent from the curves in Fig. 12 that a scatterer containing light atoms has a considerable moderating effect. For light water this effect is so large that there is no well-defined $1/E$ part at all. The materials of heavier atoms give a fairly good

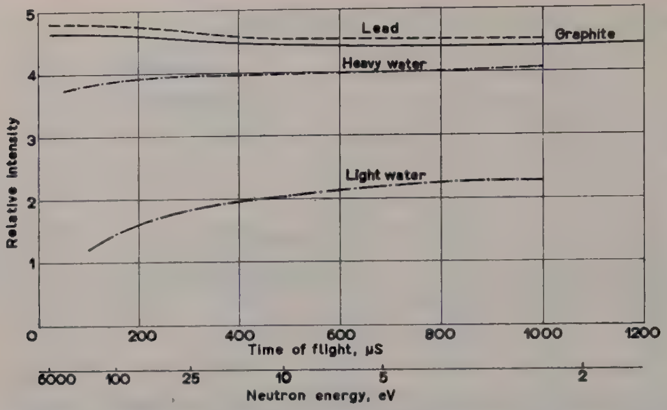

Fig. 12. The epithermal spectrum. The curves have been normalized to the same height in the thermal region.

$1/E$ spectrum in the lower epithermal region. In the region from 2 to 10 eV (at least for lead and graphite) the measured values are constant within about ±1 %, which means that the spectrum is accurately of $1/E$ shape. At higher energies there is a slight decrease in the heavy water curve, but for graphite and lead, the curves increase instead. Including all uncertainties in the measurements, this increase is estimated as 6 ± 3 %. The reason for this deviation from the $1/E$ law is probably the resonance absorption in the uranium. The resonance escape probability factor for the reactor lattice is estimated as 0.92 so the effect has the right order of magnitude.

In this connection we can also mention that the measurements described in section C 1 with a cadmium-covered graphite scatterer also showed the same deviation from the $1/E$ spectrum, though somewhat less pronounced.

The epithermal spectrum in a reactor is usually characterized by a parameter β defined from

$$\phi_{\mathrm{epi}}(E) = \frac{\beta \cdot \phi_{\mathrm{th}}}{E},$$

where ϕ_{th} is the total thermal flux. Here we relate the β value to the region between 500 and 1500 μs flight time (1.0 to 9.4 eV) where the spectrum follows the $1/E$ law closely (except for the H_2O scatterer). By relating the average pulse number in this region with the maximum pulse number in thermal region (see Fig. 13), the parameter β was obtained. In Fig. 13 we have plotted the β values obtained with different scatterers in different positions in the reactor. In the centre of the reactor the average values were

Lead	0.0450 ± 0.0015
Graphite	0.0445 ± 0.0015
Heavy water	0.0400 ± 0.0015
Light water	0.0220 ± 0.0010

The fraction of epithermal neutrons does not seem to vary very much from point to point in the reactor. Only towards the heavy water level of the reactor there is a

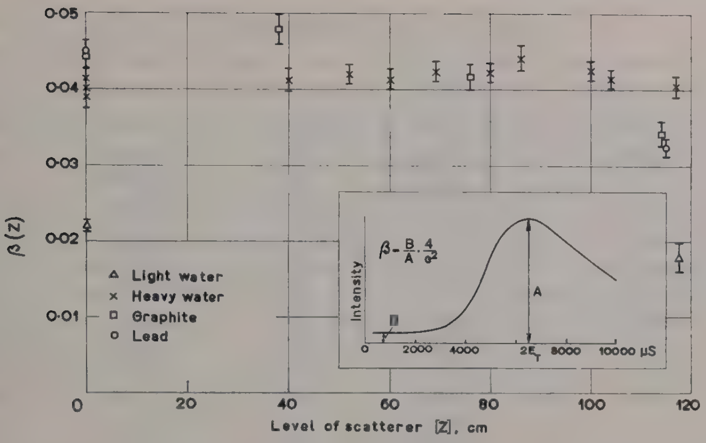

Fig. 13. The epithermal fraction, β, at different scatterer positions.

tendency for β to drop. This tendency was also found at the bottom of the reactor where the lead scatterer was used. The reason for this drop is probably neutrons which have left the core and are reflected back after some moderation.

5. *The joining region*

An energy region of special interest is that where the thermal Maxwell spectrum and the epithermal $1/E$ spectrum meet. With the present experimental set-up, this joining region could be studied in detail. After the thermal spectrum had been fitted to a Maxwell distribution as described in section C2, this distribution was subtracted from the measured data. A typical resulting curve is shown in Fig. 14. At about 0.3 eV

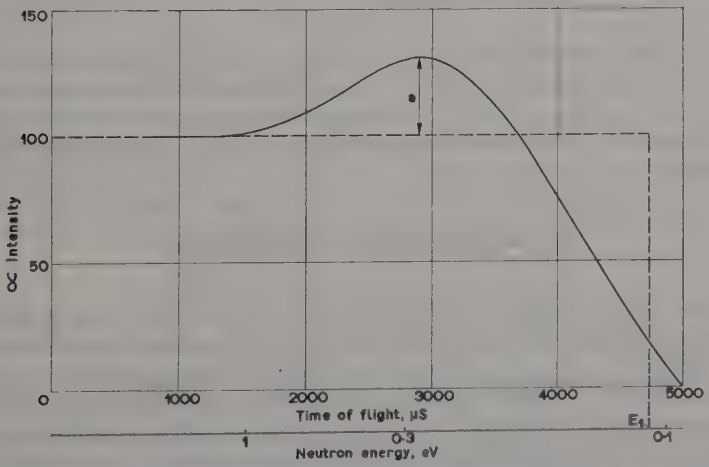

Fig. 14. A typical curve of the spectrum in the joining region obtained after subtraction of a Maxwellian distribution. Above 4000 μs the shape of the curve is rather uncertain.

Table 5. Values of a and μ.

Run no.	Scatterer	t_s (μs)	a (%)	E_1 (eV)	μ
110	Graphite	4500	30	0.108	3.6
		5000	31	0.102	3.5
		5500	31	0.098	3.3
115	Lead	4500	29	0.112	3.8
		5000	30	0.108	3.7
		5500	30	0.106	3.6
122	D_2O	4500	35	0.110	3.8
		5000	35	0.103	3.6
		5500	35	0.103	3.6
129	D_2O	4500	31	0.115	4.0
		5000	32	0.103	3.6
		5500	33	0.090	3.2

there is a bump in the curve whose maximum height above the $1/E$ level we denote a. Another parameter of interest is the effetive lower limit of the $1/E$ part referred to a $1/v$ absorber. This energy limit, E_1, is defined in Fig. 14, where the area below the measured curve is equal to the area under the rectangle with its limit at E_1. Values of E_1 and a are given in Table 5, which is based on the same measurements as Table 3. μ is the ratio between E_1 and E_T, and t_s denotes different starting times in the fitting of the Maxwell distribution.

We see that the parameter a is rather independent of t_s and of the scattering material. As an average, we may adopt (32 ± 4) %. The values of μ, however, scatter considerably. This is not unexpected because the value of E_1 must be very sensitive to the exact shape of the curve resulting from subtraction of the Maxwell distribution. Any deviation from the Maxwell shape (even though it must be small, as we found in section C2) would influence the value of E_1 very much. As an average value of μ we adopt 3.6 ± 0.4.

Some special measurements with high resolution and good statistical accuracy were made in the energy region 0.2 to 10 eV in order to see whether there was any fine-structure in the neutron spectrum. No irregularities could be found which were significantly outside the statistical uncertainty of ± 1 % obtained with a channel width of 30 μs.

D. Foil and counter measurements

1. *General*

The chopper work described above has been supplemented with several foil and counter measurements. The main purpose of these measurements was to get a comparison between the spectrum in the chopper beam and the undisturbed spectrum in the reactor channel. Further we wanted to have a check on the general reliability of the chopper results. Cadmium ratio measurements using a thin BF_3 counter in the chopper beam were a good over all test of the apparatus. For comparison of the thermal spectra, lutetium and copper foils were activated, and cadmium ratios of gold and copper were measured to relate the epithermal spectra to each other.

2. *Cadmium ratio measurements with thin boron counter*

Cadmium ratio measurements were made in the chopper beam with a boron trifluoride counter. The diameter of the counter was 3 cm and it was filled to a pressure of 30 mm Hg with enriched (94 %) BF_3 and with argon to a total pressure of 600 mm Hg. It was placed about 80 cm above the top of the reactor. Cadmium sheets 1.1 mm thick were used. The scatterer was either graphite or heavy water. In addition to the normal reactor conditions, measurements were also made when one of the six uranium rods closest to the central channel had been removed (see Fig. 7), even though this did not correspond to any chopper measurements. The reactor power at the experiments was 400 W and the moderator temperature was 300°K.

The cadmium ratio R_{Cd} for a $1/v$ absorber in a spectrum with a Maxwell and a $1/E$ distribution is

$$R_{\mathrm{Cd}}=\frac{0.94\,(1/\sqrt{E_T})\,\frac{1}{2}\sqrt{\pi}+2\,\beta/\sqrt{E_1}}{2\,\beta/\sqrt{E_{\mathrm{C}}}}.$$

Here the factor 0.94 (with uncertainty ± 0.01) takes into account the distortion of the spectrum because of 4.8 m air between the scatterer and the counter. E_T is put equal to 0.0284 ± 0.0006 eV (corresponding to the neutron temperature $300+29$°K) and $E_1=\mu E_T=0.102\pm0.011$ eV (according to Table 5). E_{C} is the effective cadmium cut-off energy as seen by a $1/v$ counter. It has been determined directly by chopper measurements to have the values 0.0490 ± 0.0015 and 0.0470 ± 0.0015 for graphite and heavy water respectively.

The results from the counter measurements are given in Table 6. We see that the values obtained with six rods agree very well with the chopper measurements as described in section C4. This gives us some confidence in the reliability of the measurements. From Table 6 we see also, as expected, a fairly large change in the epithermal fraction when one of the central uranium rods is removed.

3. *Lutetium foil measurements*

Measurements with lutetium foils were made to compare the shape of the thermal neutron spectrum in the beam with the more or less isotropic thermal spectrum in the central channel without scatterer. The use of lutetium has been described by Price [6]. Lutetium has two stable isotopes: Lu^{175} (97.4 %) and Lu^{176} (2.6 %). The latter exhibits a resonance at 0.142 eV, so its cross section deviates strongly from the $1/v$ law in the thermal region. The isotope Lu^{177} which is formed by the activation has a half-life of 6.7 days and a maximum beta energy of 0.5 MeV. It is therefore very suitable to use in activation measurements. Also the other isotope formed by activa-

Table 6. R_{Cd} and β from BF_3 counters.

Scatterer	Six rods		Five rods	
	R_{Cd}	β	R_{Cd}	β
Heavy water	45.5 ± 0.5	0.0393 ± 0.0012	49.8 ± 0.5	0.0357 ± 0.0012
Graphite	42.8 ± 0.5	0.0427 ± 0.0012	46.3 ± 0.5	0.0394 ± 0.0012

tion, Lu^{176m}, is convenient for measurements, its half-life being 3.65 hours and maximum beta energy 1.2 MeV. We first investigated whether it would be possible to use this isotope, which presumably has a $1/v$ cross section, as the $1/v$ standard. However, the cadmium ratio was very low (only 1.9 in our case) which would make it difficult to correct for the epithermal activity. So we chose copper as the $1/v$ standard to use with the isotope Lu^{176}, the cadmium ratio of which was about 95 (in the beam from the D_2O scatterer with one rod removed).

The lutetium foils were made by spreading a mixture of Lu_2O_3 powder and an organic glue as uniformly as possible on thin aluminium discs. It is necessary to use thin foils in our case when monodirectional and isotropic fluxes are compared. Therefore, our foils contained only about 1 mg lutetium per cm^2.

The copper and lutetium foils were first irradiated in the chopper beam with the reactor at 1 MW power level, and later in the middle of the central channel (without scatterer) at 4 kW. Two bare and one cadium covered foil of each kind were used, and the foils were the same in both measurements. The activities were measured with a beta scintillation counter.

The results can be expressed in the ratios of the normalized counting rates for the lutetium and copper foils for subcadmium neutrons. This turned out to be 25.4 ± 0.4 in the beam and 24.4 ± 0.4 in the middle of the reactor. If both spectra are assumed to be Maxwellian this would mean 10 ± 8 degrees higher neutron temperature of the beam. This must be corrected for the difference in moderator temperature between the two measurements which was 10 degrees. Thus we find that the neutron temperature in the beam is the same within ± 8 degrees as that in the central channel of the reactor.

4. *Cadmium ratio measurements with gold and copper foils*

To compare the epithermal spectra in the chopper beam and in the central channel (without scatterer) the cadmium ratios of thin gold and copper foils were measured in the reactor. Bare and cadmium-covered foils were irradiated at the same time hanging at 10 cm distance from each other. The cadmium thickness was 0.5 mm and the area of the cadmium cover was varied in steps from 12 to 50 cm^2 in order to allow extrapolation to zero cover size. These measurements were also made during that period mentioned in section D.2 when there were only five instead of six uranium rods close to the central channel. The power level was 4 kW and the moderator temperature 300°K, corresponding to $E_T = 0.0284 \pm 0.0006$ eV. The cadmium ratio for gold was found to be 2.48 ± 0.03 and for copper 21.3 ± 0.3.

The resonance integral of copper was assumed to be 2.82 ± 0.10 *b* (from recent measurements by R. Dahlberg). For the resonance integral of gold, we have according to earlier work, a value of 1490 ± 40 *b* [7].

After correction for self-absorption and non-$1/v$ thermal absorption cross section the β value obtained for gold is 0.0383 ± 0.0015 and for copper 0.0387 ± 0.0020. So inside the reactor with five central rods the epithermal fraction can be put equal to 0.0385 ± 0.0015. Comparing this with the results given in Table 6 from measurements in the reactor beam, we find that there is good agreement with the result with a graphite scatterer and five uranium rods which was 0.0394 ± 0.0012. Using the results in Table 6 the "foil value" 0.0385 can be transferred to 0.0420 ± 0.0015 valid for six central rods, which we choose as a final β-value.

Conclusions

From the measurements described above we can draw the following conclusions.

1. The counter and foil measurements show that the beam spectrum as seen by the chopper from a graphite or lead scatterer is very closely the same as in the central channel without scatterer. Therefore, it is probably also rather similar to the average neutron spectrum in the reactor moderator.

2. The thermal neutron spectrum has very closely a Maxwellian shape. The neutron temperature in the beam is 29 ± 6 degrees higher than the moderator temperature, and it is the same within ± 8 degrees as the neutron temperature in the empty central channel. Thus the neutron temperature in the reactor is probably 29 ± 10 degrees higher than the moderator temperature.[1] (This is somewhat lower than what Larsson *et al.* [8] found from experiments in a different beam.) The neutron temperature does not vary much inside the reactor.

3. The epithermal spectrum deviates slightly from the $1/E$ law due to the resonance absorption in uranium. To our knowledge, no such deviation has been observed before. It may lead to appreciable corrections in experiments where a $1/E$ spectrum is usually assumed. The β value defined from the 1–10 eV region in the centre of the reactor is 0.0420 ± 0.0015.

4. When the Maxwell spectrum has been subtracted from the total spectrum, there is (on a plot in timescale) a bump in the spectrum. It rises to a maximum of 32 ± 4 % above the $1/E$ level. The effective starting point of the $1/E$ spectrum is at (3.6 ± 0.4) E_T. A similar increase of the spectrum in the joining region can also be seen in earlier work [2], [4].

AB Atomenergi, Department for Reactor Physics, Stockholm, Sweden.

REFERENCES

1. Poole, M. J., Nelkin, M. S., and Stone, R. S., Progr. Nucl. En. Ser. 1, *2* (1958).
2. Campbell, C. G., Freemantle, R. G., and Poole, M. J., Proc. Second Int. Conf. on the Peaceful Uses of Atomic Energy *16*, p. 233 (1958).
3. Mostovoi, V. I., Dikarev, V. S., Egiazarov, M. B., and Saltykov, Y. S., Proc. Second Int. Conf. on the Peaceful Uses of Atomic Energy *16*, p. 254 (1958).
4. Stone, R. S. and Slovacek, R. E., Nucl. Sci. Eng. *6*, 466 (1959).
5. Egelstaff, P., Proc. Int. Conf. on the Peaceful Uses of Atomic Energy *4*, p. 70 (1955).
6. Price, G. A., Reactor Sci. *10*, 314 (1959).
7. Jirlow, K. and Johansson, E., Reactor Science *11*, 101 (1960).
8. Larsson, K. E., Stedman, R., and Palevsky, H., J. Nucl. En. *6*, 222 (1958).

---

[1] This value is 7 degrees higher than the preliminary one reported at the EAES symposium at Risø and at the ANS meeting in Chicago.

Tryckt den 22 november 1960

Uppsala 1960. Almqvist & Wiksells Boktryckeri AB